Activation of the NFAT–Calcium Signaling Pathway in Human Lamina Cribrosa Cells in Glaucoma

Mustapha Irnaten,[1] Alexander Zhdanov,[2] Deirdre Brennan,[3] Thomas Crotty,[4] Abbot Clark,[5] Dmitri Papkovsky,[2] and Colm O'Brien[1,4]

[1]Ophthalmology, Mater Misericordiae University Hospital, Dublin, Ireland
[2]School of Biochemistry & Cell Biology, University College Cork, Cork, Ireland
[3]Department of Anatomy, University College Dublin School of Medicine, Health Sciences Centre, University College Dublin, Belfield, Dublin, Ireland
[4]School of Medicine and Medical Science, University College Dublin, Dublin, Ireland
[5]The North Texas Eye Research Institute, University of North Texas, Health Science Center, Fort Worth, Texas, United States

Correspondence: Colm O'Brien, 60 Eccles Street, Mater Misericordiae University Hospital, Dublin 7, Ireland;
cobrien@mater.ie.

Submitted: July 1, 2017
Accepted: January 8, 2018

Citation: Irnaten M, Zhdanov A, Brennan D, et al. Activation of the NFAT–calcium signaling pathway in human lamina cribrosa cells in glaucoma. *Invest Ophthalmol Vis Sci*. 2018;59:831–842. https://doi.org/10.1167/iovs.17-22531

Purpose. Optic nerve cupping in glaucoma is characterized by remodeling of the extracellular matrix (ECM) and fibrosis in the lamina cribrosa (LC). We have previously shown that glaucoma LC cells express raised levels of ECM genes and have elevated intracellular calcium ($[Ca^{2+}]_i$). Raised $[Ca^{2+}]_i$ is known to promote proliferation, activation, and contractility in fibroblasts via the calcineurin–NFAT (nuclear factor of activated T-cells) signaling pathway. In this study, we examine NFAT expression in normal and glaucoma LC cells, and investigate the effect of cyclosporin A (CsA, a known inhibitor of NFAT activity) on $[Ca^{2+}]_i$ and ECM gene expression in normal and glaucoma LC cells.

Methods. $[Ca^{2+}]_i$ was measured with dual-wavelength Ca^{2+} imaging and confocal microscopy using Fura-2-AM and Fluo-4 under physiological isotonic and hypotonic cell stretch treatment. Human donor LC cells were cultured under normal physiological conditions or using a glaucoma-related stimulus, oxidative stress (H_2O_2, 100 μM), for 6 hours with or without CsA. NFATc3 protein levels were examined using Western blot analysis. Profibrotic ECM gene transcription (including transforming growth factor-β1 [TGFβ1], collagen 1A1 [Col1A1], and periostin) was analyzed using quantitative real time RT-PCR.

Results. Basal and hypotonic cell membrane stretch-induced $[Ca^{2+}]_i$ were significantly ($P < 0.05$) elevated in glaucoma LC cells compared to normal controls. There was a significant delay in $[Ca^{2+}]_i$ reuptake into internal stores in the glaucoma LC cells. NFATc3 protein levels were increased in glaucoma LC cells. CsA (10 μM) significantly inhibited the H_2O_2-induced expression of NFATc3 in normal and glaucoma LC cells. CsA also reduced the H_2O_2-induced NFATc3 dephosphorylation (and nuclear translocation), and also suppressed the H_2O_2-induced elevation in profibrotic ECM genes (TGFβ1, Col1A1, and periostin), both in normal and in glaucoma LC cells.

Conclusions. Intracellular Ca^{2+} and NFATc3 expression were significantly increased in glaucoma LC cells. CsA reduced the H_2O_2-induced enhancement in NFATc3 protein expression and nuclear translocation and the profibrotic gene expression both in normal and in glaucoma LC cells. Therefore, targeting the calcineurin–NFATc3 signaling pathway may represent a potential avenue for treating glaucoma-associated LC fibrosis.

Keywords: glaucoma, lamina cribrosa, extracellular matrix, intracellular calcium, transcription factors

Glaucoma is the most common cause of treatable visual impairment in the developed world.[1] It is a chronic neurodegenerative disease characterized by cupping and pallor of the optic nerve head (ONH) and by the slow progressive death of retinal ganglion cells. Histologically, there is remodeling of extracellular matrix (ECM) in the lamina cribrosa (LC) region leading to fibrosis of the LC connective tissue,[2,3] which is driven in part by profibrotic growth factors such as transforming growth factor-β (TGFβ).[4,5]

Fibrosis is attributed to excessive ECM accumulation that ultimately impairs the connective tissues.[6] External stimuli such as oxidative stress, mechanical stretch, and growth factors cause fibroblasts to change their phenotype and differentiate into myofibroblasts.[7,8] The main features of myofibroblast differentiation are the disproportionate increase in the expression of structural ECM proteins, matricellular proteins, smooth muscle α-actin (αSMA), and TGFβ[7,9,10] LC cells have many characteristics of myofibroblasts including the expression of α-SMA, and a marked expression of profibrotic genes and proteins (collagen 1A1 [Col1A1], periostin, fibronectin) upon stimulation with cyclic stretch,[11] oxidative stress,[12] and endothelin.[13] In physiological wound healing, the activity of myofibroblasts is terminated when the tissue is repaired and they later disappear from the wound by apoptosis.[14] In pathologic wound healing,

however, myofibroblast activity (associated with a lack of apoptosis) persists and leads to deposition of excessive ECM components in which normal tissue is replaced by permanent fibrotic scar tissue,[15] such as that seen in the LC in glaucoma.[2,3]

Chronic elevation of intracellular calcium ($[Ca^{2+}]_i$) levels activates downstream Ca^{2+}-dependent signaling pathways that can mediate maladaptive ECM remodeling often leading to fibrosis.[16] For example, in the heart, one such pathway is regulated by the Ca^{2+}-calmodulin–dependent phosphatase calcineurin, which has been shown to be crucial for pathologic cardiac hypertrophy and fibrosis.[17,18] Increased $[Ca^{2+}]_i$ activates a serine/threonine phosphatase, calcineurin, that binds to Ca^{2+} and calmodulin, leading to dephosphorylation of the transcription factor, nuclear factor of activated T-cells (NFAT) in the cytoplasm. Dephosphorylated NFAT translocates into the nucleus where it complexes with other transcription factors to regulate and drive hypertrophic gene transcription,[18–20] thus providing a direct link between $[Ca^{2+}]_i$ signaling and gene expression.[21,22] Cyclosporin A (CsA) is a calcineurin inhibitor that blocks NFAT dephosphorylation in the cytoplasm, precluding its movement to the nucleus and thereby preventing increased gene transcription levels of profibrotic ECM gene production.[18,23,24] In addition, when Ca^{2+} entry is blocked or calcineurin activity is inhibited, NFAT is rephosphorylated by NFAT kinases and rapidly leaves the nucleus, and NFAT-dependent gene expression is terminated.[25] CsA is an immunosuppressive and antifibrotic agent used to treat a variety of systemic immunosuppressive conditions including rheumatoid arthritis[26,27] and also for ocular inflammation,[28] where it has been shown to inhibit fibrosis and inflammatory cell infiltration in conjunctivitis,[29] and in dry eye treatment.[30]

We have previously shown elevated baseline and hypotonic cell membrane stretch-induced increase in $[Ca^{2+}]_i$ in glaucoma LC cells.[31] Our experimental results, using different pharmacologic Ca^{2+} inhibitors (verapamil [L-type Ca^{2+} channel blocker] and 2-APB [store-operated Ca^{2+} channel blocker]), showed that glaucoma LC cells also have higher baseline levels of Ca^{2+}-dependent potassium (maxi-K^+) ion activity.[31] Our results also showed that both sources of cytosolic Ca^{2+} elevation (Ca^{2+} entry and release from intracellular stores) contribute to the abnormally elevated $[Ca^{2+}]_i$ in glaucoma LC cells.[31] Also, the maxi-K activity was sensitive to stretch as gadolinium (stretch-activated Ca^{2+} entry channel blocker) significantly reduced the hypotonic stretch–induced increase in maxi-K activity in normal LC cells.[32] In addition, we found that glaucoma LC cells have markers of oxidative stress and mitochondrial dysfunction,[12] and express raised levels of several ECM genes such as periostin, collagen 1A1, and thrombospondin-1.[33] In the current study, we explore the NFAT–calcineurin signaling pathway and investigate the effect of CsA on ECM gene expression in normal and glaucoma LC cells exposed to oxidative stress.

Materials and Methods

Experimental Reagents and Solutions

Unless otherwise stated, reagents including chemicals used were analytical grade and obtained from Sigma (Dublin, Ireland).

LC Cell Culture

LC cells were isolated and cultured after retrieval from human eye donors. They were donated to us by Alcon Labs (Fort Worth, TX, USA), approximately every 12 months. They were routinely characterized for markers such as α-SMA stain while being negative for glial fibrillary acidic protein (GFAP) (an astrocyte marker) and ionized Ca^{2+} binding adapter molecule 1 (Iba1) (a microglial marker), as previously described.[31,34] Briefly, freshly thawed human LC cells were obtained from age-matched healthy donor eyes with no history of glaucoma, ocular disease, or other neurologic diseases ($n = 7$ eye donors) and from donors with confirmed glaucoma ($n = 7$ eye donors). Newly characterized LC cells were cultured and maintained at 37°C with 95% humidified air atmosphere and 5% CO_2 in low-glucose Dulbecco's modified Eagle's medium (DMEM) containing 10% (vol/vol) fetal bovine serum (FBS) and antibiotics. Culture medium was changed twice weekly; cells were maintained in full medium until reaching 80% to 90% confluence and passaged as needed. Passages 4 through 8 were used for experiments.

Hypotonic Cell Stretch and Hydrogen Peroxide Treatments of Lamina Cribrosa Cells

We investigated the effect of two glaucoma-related stimuli (hypotonic cell membrane stretch and oxidative stress) on $[Ca^{2+}]_i$ and downstream profibrotic ECM gene transcription. Hypotonic cell membrane stretch involved rapid replacement of the physiological isotonic solution (osmolarity: 323 ± 6 mOsm) consisting of (mM): 120 NaCl, 6 KCl, 1 $MgCl_2$, 2 $CaCl_2$ 5.4 HEPES, and 80 D-mannitol with hypotonic solution (osmolarity: 232 ± 8 mOsm), which was prepared by omitting D-mannitol from the isotonic solution. Oxidative stress involved hydrogen peroxide (H_2O_2, 100 μM) incubation for 6 hours, looking at the effects on NFATc3 and profibrotic genes such as periostin, Col1A1, and TGFβ1 transcription in normal and glaucoma LC cells. To evaluate the effect of CsA on profibrotic gene transcription and NFATc3 expression, both normal and glaucoma LC cells were cultured in DMEM containing CsA (10 μM) overnight before being harvested for experiments. CsA was dissolved in vehicle control ethanol and at the matched concentration (10 μM); the vehicle control had no effect on either NFATc3 protein expression or its dephosphorylation or profibrotic gene transcription. Dose–response experiments under both hypotonic cell membrane stretch and oxidative stress effects on LC cell viability have been performed, and the hypo-osmolarity (232 mOsm) and H_2O_2 (100 μM) used had no effect on cell viability.[31,32] Also, the cytotoxic effect of CsA was tested and no effect was observed on LC cell viability at the concentration used (10 μM) (results not shown).

Calcium Imaging

The dual-wavelength ratiometric Ca^{2+} imaging technique, using the membrane-permeable ester of the Ca^{2+}-sensitive fluorescent dye Fura-2-AM to measure $[Ca^{2+}]_i$ changes, is a standard technique extensively used by numerous laboratory groups worldwide mostly based on the work by Grynkiewicz et al.[35] In the eye, this protocol has been used to measure the $[Ca^{2+}]_i$ changes in RPE cells[36] and trabecular meshwork (TM) cells.[37] We previously used Fura-2-AM to record the real-time $[Ca^{2+}]_i$ changes in LC cultured cells subjected to hypotonic and cyclic stretch.[31] In brief, confluent LC cells were loaded with 5 μM Fura-2-AM for 45 minutes in darkness at room temperature, washed twice, and kept in Ca^{2+}-free physiological isotonic solution (osmolarity was at 323 ± 6 mOsm), and then the coverslip was mounted on the stage of an inverted epifluorescence microscope (Diaphot 200; Nikon, Toyko, Japan). A monochromator dual-wavelength enabled alternative excitation at 340 and 380 nm, whereas the emission fluorescence was monitored at 510 nm with an Okra Imaging camera

Investigative Ophthalmology & Visual Science

Table. Profibrotic Gene Primers Used for Real-Time RT-PCR

Gene	Forward	Reverse
TGFβ1	GCAGTGGCTGAACCAAGGA	GCAGTGAGCGCTGAATCGA
Periostin	GAAAGGGAGTAAGCAAGGGAG	ATAATGTCCAGTCTCCAGGTTG
Col1A1	ACGAAGACATCCCACCAATC	ATGGTACCTGAGGCCGTTC
GAPDH	CTGGGACGACATGGAGAAAA	AAGGAAGGCTGGAAGAGTGC

(Hamamatsu, Japan). The images of multiple cells collected at each excitation wavelength were processed using Openlab2 software (Improvision system, London, UK) to provide ratios of Fura-2-AM fluorescence from excitation at 340 nm to that from excitation at 380 nm (F340/F380). All experiments were corrected for background fluorescence before the Fura-2-AM ratio was calculated. The $[Ca^{2+}]_i$. was obtained according to the equation provided by Grynkiewicz et al.[35]:

$$\left[Ca^{2+}\right]_i = K_d \frac{\left(F_{380\,Ca\,free} \cdot \left(R_0 - R_{min}\right)\right)}{\left(F_{380\,Ca\,max} \cdot \left(R_{max} - R_0\right)\right)}$$

where the dissociation constant (K_d) was assumed to be 225 nM, R_{min} is the ratio of fluorescence measured at 340 nm (F_{340}) over 380 nm (F_{380}) in a "nominally" Ca^{2+}-free solution. R_{max} is the ratio of fluorescence measured at 340 nm over 380 nm.

Fluorescence traces shown represent $[Ca^{2+}]_i$ values that are representative of at least 50 to 80 cells and are presented as $[Ca^{2+}]_i$ fluorescence ratio (340/380). The histograms (average data from seven age-matched normal eye donors and seven glaucoma patients) are presented as the absolute changes in $[Ca^{2+}]_i$. During the experiments, which typically take 20 minutes, the pH and temperature are continuously monitored and maintained constant.

To study the release of Ca^{2+} from internal stores, the LC cells were washed twice and kept in Ca^{2+}-free isotonic solution, and ethylene glycol-bis(β-aminoethyl ether)-N,N,N′,N′-tetraacetic acid (EGTA) (5 mM) was added to remove the residual external Ca^{2+}. Thapsigargin (TG) (1 μM) was added to block the sarcoendoplasmic reticulum Ca^{2+}-ATPase (SERCA) pumps, inducing a complete depletion of Ca^{2+} from intracellular stores. The isotonic solution was then replaced with hypotonic solution, and $CaCl_2$ (2 mM) was added extracellularly to facilitate Ca^{2+} influx via the store-operated channels that opened because of Ca^{2+} store depletion.

Cell Lysate Preparation and Western Blot Analysis

Normal and glaucoma LC cells were plated in T75-mm tissue culture dishes and grown until 90% confluent and placed in serum-free medium for 24 hours. The serum-free medium was then removed and cells were subjected to oxidative stress using H_2O_2 for 6 hours at 37°C with or without CsA treatment. The reaction was stopped by removal of the medium and introduction of ice-cold phosphate-buffered saline (PBS). The crude cell lysate was collected using radio immuno-precipitation assay (RIPA) buffer containing protease inhibitor cocktail, and then the cells were incubated on ice for 5 minutes and subsequently centrifuged for 15 minutes at 17968*g* at 4°C. The cleared supernatant was collected and the protein concentration was quantified using the Bradford method. Protein extracts (20 μg) were electrophoresed on 10% polyacrylamide-SDS gels and transferred to a nitrocellulose membrane. For control and treated samples, equal amounts of protein were loaded in the SDS-PAGE. After blocking, membranes were incubated overnight at 4°C with polyclonal antibodies for total (tNFATc3) and phosphorylated NFATc3 (pNFATc3) (1:500; Santa Cruz, Heidelberg, Germany). After washing, membranes were incubated for 1 hour at room temperature with anti-rabbit IgG-horseradish peroxidase–conjugated secondary antibody (1:10,000; Cell Signaling, Dublin, Ireland). Membranes were reprobed with either anti-β-actin or GAPDH antibody (Cell Signaling) as loading controls. The blots were then processed according to standard protocols using ECL detection system (Fisher Scientific, Dublin, Ireland).

RNA Extraction and Quantitative Real-Time PCR

Total RNA from LC cells was extracted with Tri-Reagent (Life Technologies, Dublin, Ireland); total RNA was converted to cDNA using enhanced avian reverse transcriptase (eAMV), and 2 μg total RNA was used for first-strand synthesis with oligo-dT, deoxynucleotides (dNTPs), and primers. The following genes were analyzed using primers designed on qPrimerDepot and manufactured by Sigma: TGFβ1, Col1A1, and periostin (Table). To quantify cDNA expression levels, quantitative RT-PCR was performed using a Rotorgene 3000 Real-Time PCR Thermocycler (Labortechnik, Wasserburg, Germany). The cDNA was assayed in triplicate using QuantiTect SYBR Green PCR Master Mix (Qiagen, Manchester, UK). Data are presented as relative fold change of expression of the housekeeping gene *Gapdh* using the formula $2^{-\Delta\Delta CT}$ in which CT is the cycle threshold number.[38]

Immunofluorescence Microscopy

To demonstrate that CsA prevents the oxidative stress-induced NFATc3 nuclear translocation, we used immunofluorescence microscopy. The primary human LC cells (passages 4–8) were seeded and grown on the Nunc Lab-Tek II Chamber Slide System (Thermo Scientific, Dublin, Ireland) in DMEM growth medium until confluence was reached. Control nontreated LC cells treated with H_2O_2 and LC cells pretreated with CsA were used. Cells were fixed in 100% ice-cold methanol for 5 minutes, permeabilized in 0.05% Triton X-100, blocked in 10% goat serum, and rinsed three times with PBS. Cells were incubated overnight at 4°C with 1:50 dilution of mouse monoclonal p-NFATc3 (sc-365785; Santa Cruz) followed by three washes for 5 minutes with PBS, and then incubated in the dark for 1 hour at room temperature with 1:250 dilution goat anti-mouse IgG-Fab–specific FITC conjugate (F2653 Sigma Aldrich Ireland) followed by three washes for 5 minutes. Hoechst 33342 (Thermo Scientific) was used as a nuclear counterstain. Images were captured using an Olympus BX51 fluorescent microscope and associated CellSens software (Olympus, Cardiff, UK).

Confocal Microscopy

LC cells were seeded on MatTek glass bottom Petri dishes (MatTek, Ashland, MA, USA) at 1500 cells/cm^2 and grown in DMEM overnight. Loading with fluorescent sensor Fluo-4 FM (2.5 μM) was performed for 30 minutes in Opti-MEM medium in the dark; then the medium was replaced with fresh DMEM and cells were incubated for 30 minutes prior to microscopy. Confocal fluorescence imaging was conducted on the Olympus FV1000 confocal laser scanning microscope with controlled

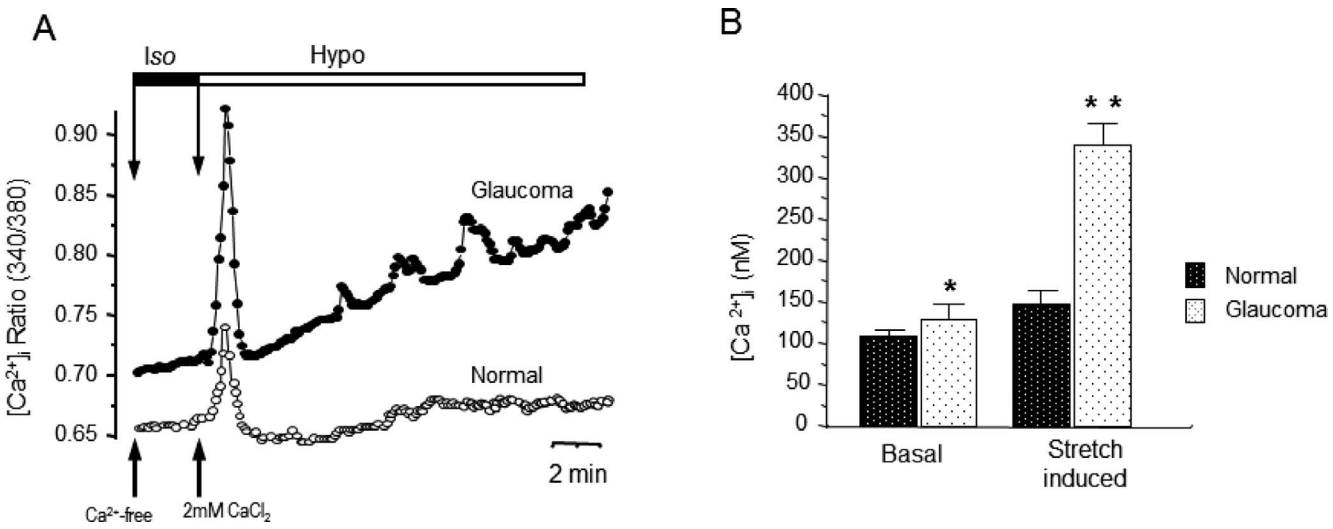

Figure 1. Elevated basal and hypotonic stretch-induced intracellular Ca^{2+} in glaucoma LC cells. (**A**) Representative time tracings of the $[Ca^{2+}]_i$ ratio (340/380) in Fura-2-AM–loaded normal (○) and glaucoma (•) LC cells in isotonic solution (Iso) followed by hypotonic stretch (Hypo) in the presence of 2 mM extracellular Ca^{2+}. The changes in $[Ca^{2+}]_i$ were taken from measuring peak values and expressed as the change in fluorescence ratio from basal levels and determined for each experiment. The *first arrow* indicates the start of experiment and the *second arrow* the timing of osmolarity change. (**B**) Increase of mean cytosolic Ca^{2+} in Fura-2-AM–loaded LC cells ($^*P < 0.05$, $^{**}P < 0.01$, $N = 11$ different experiments, $n = 80$ cells for three different LC cell strains obtained from normal donors and three different LC cell strains from glaucoma patients). Note the higher level of intracellular Ca^{2+} of both basal and hypotonic stretch induced in glaucoma.

CO_2, humidity, and temperature. The Fluo-4 probe was excited at 488 nm (10% of maximal laser power) with emission collected at 500 to 540 nm. Changes in cytosolic Ca^{2+} levels in cells upon treatment with H_2O_2 (100 μM) were compared to that in cells pretreated overnight with CsA (10 μM). In all experiments, differential interference contrast (DIC) and fluorescence images were collected kinetically with a ×60 oil immersion objective in 12 planes using 0.25-μm steps and 4-minute intervals. The resulting z-stacked images were analyzed using FV1000 Viewer software (Olympus), Excel (Microsoft Corporation, Redmond, WA, USA), and Adobe Photoshop and Illustrator (Adobe Systems, Inc., San Jose, CA, USA).

Statistical Analysis

Data were expressed as means of independent experiments, with SE error bars, or representative individual experiments. Statistical significance was analyzed by Student's *t*-test (2-tailed; paired or unpaired as appropriate) for comparison between two groups and by 1-way analyses of variance (ANOVA) with Tukey-Kramer posttest for multiple comparisons. $P < 0.05$ was taken as the level of significance ($^*P < 0.05$, $^{**}P < 0.01$). *N* refers to the number of eye donors, and *n* refers to the number of the cells in one experiment. Calculations were performed by the Origin 7.0 software (OriginLab, Stoke Mandeville, Bucks, UK). Densitometric analysis of Western blots was performed using Gene Tools software (Syngene, Cambridge, UK). For confocal microscopy experiments, differences in Fluo-4 intensities were analyzed using the Mann-Whitney *U* test.

Results

Basal and Hypotonic Stretch $[Ca^{2+}]_i$ Levels Are Elevated in Glaucoma LC Cells

Our recent work reported the effect of hypotonic stretch on $[Ca^{2+}]_i$ in normal LC cells.[39] Here we wished to compare the basal and hypotonic cell membrane stretch-induced changes in $[Ca^{2+}]_i$ levels between normal and glaucoma LC cells. Using radiometric dual-wavelength imaging on Fura-2-AM–loaded LC cells, basal $[Ca^{2+}]_i$ was first measured in isotonic solution for 5 minutes to obtain a stable baseline, and then hypotonic solution was applied to create hypotonic cell membrane stretch, as glaucoma-related stimulus, and $[Ca^{2+}]_i$ measurement was recorded for 20 minutes. As shown in Figure 1, the basal $[Ca^{2+}]_i$ was significantly greater in glaucoma LC cells (129.18 ± 8.22 nM) versus normal LC cells (108 ± 4.96 nM) ($n = 9$ independent experiments, 80 cells; $^*P < 0.05$). On average, the hypotonic stimulus evoked an $[Ca^{2+}]_i$ increase to 153.46 ± 21.29 nM in normal LC cells and to 339.5 ± 25.6 nM in glaucoma LC cells. The average peak amplitude in response to hypotonic stretch of cells from seven experiments obtained from seven normal and seven glaucoma eye donors was significantly greater in the glaucoma LC cells ($P < 0.01$).

Delayed Reuptake of Intracellular Ca^{2+} Stores in Glaucoma LC Cells

Having shown that Ca^{2+} entry results in a large increase in $[Ca^{2+}]_i$ in glaucoma cells (Fig. 1), we next examined whether the extracellular Ca^{2+} is part of the abnormally elevated levels of $[Ca^{2+}]_i$ found in glaucoma LC cells.

As shown in Figure 2, we experimentally separated intracellular Ca^{2+} release from extracellular Ca^{2+} influx. Ca^{2+} influx was measured in cells loaded with Fura-2-AM. At time 0, the cells were bathed in Ca^{2+}-free isotonic standard solution with 2 mM EGTA (to chelate the residual extracellular Ca^{2+}) and 1 μM TG (to block SERCA pumps, inducing a complete depletion of Ca^{2+} from intracellular stores). As a result, $[Ca^{2+}]_i$ transiently increased and was followed by a return to low baseline levels in both normal and glaucoma LC cells (Figs. 2A, 2B). However, in normal LC cells, the $[Ca^{2+}]_i$ returned to basal level within 2 minutes, while the return to baseline took 12 to 14 minutes in glaucoma LC cells (Figs. 2A–C). When $[Ca^{2+}]_i$ was stable again, the extracellular medium was replaced by hypotonic solution and extracellular $CaCl_2$ (2 mM) was added, resulting in an influx of Ca^{2+} via Ca^{2+} entry channels. As shown in Figure 2B, the rise of $[Ca^{2+}]_i$ after changing the medium to hypotonic solution and reintroducing extracellular Ca^{2+} was

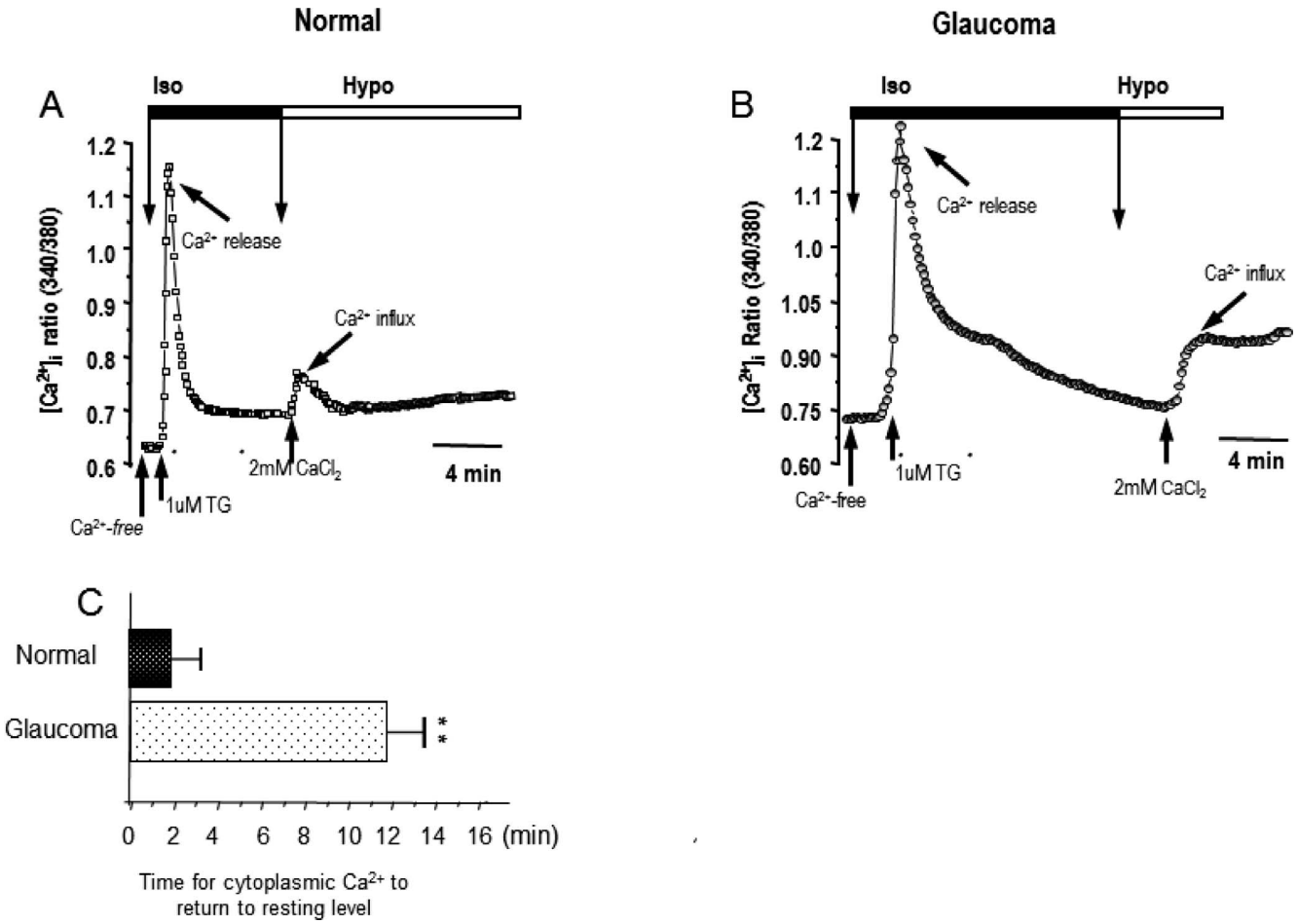

Figure 2. Effect of thapsigargin on intracellular Ca^{2+} in LC cells. (**A**) Normal LC cells and (**B**) glaucoma LC cells. Representative time tracings of cytosolic Ca^{2+} ratio in Fura-2-AM–loaded LC cells in isotonic solution in the presence of thapsigargin (TG) (1 μM) followed by removal of TG and application of hypotonic solution in the presence of 2 mM extracellular Ca^{2+}. The *first arrow* indicates the start of experiment, in which the cells were bathed in Ca^{2+}-free isotonic standard solution with 2 mM EGTA (to chelate the residual extracellular Ca^{2+}), and 1 μM TG (to block SERCA pumps and to deplete intracellular Ca^{2+} stores). Note the $[Ca^{2+}]_i$ transient increase followed by a return to low baseline level in both normal and glaucoma LC cells. However, in normal LC cells, $[Ca^{2+}]_i$ returned to basal level within 2 minutes, while the return to baseline took 12 to 14 minutes in glaucoma LC cells. Then, the extracellular medium was replaced by hypotonic solution and extracellular $CaCl_2$ (2 mM) was added. Note that the rise of $[Ca^{2+}]_i$ after changing the medium to hypotonic solution and reintroducing extracellular Ca^{2+} is significantly greater in glaucoma LC cells ($P < 0.01$), and no recovery to baseline levels was observed over the time course studied in the glaucoma LC cells. Reported data are representative of seven experiments (72 cells for one set of experiments, $N = 7$ normal and glaucoma LC cell donors). Note a significant delayed return to baseline level of $[Ca^{2+}]_i$ in glaucoma LC cells compared to normal control LC cells (**$P < 0.01$). (**C**) Delayed time for cytoplasmic Ca^{2+} to return to baseline levels in normal and glaucoma LC cells.

significantly greater in glaucoma LC cells ($P < 0.01$), and no recovery to baseline levels was observed over the time course studied in the glaucoma LC cells (Fig. 2C).

Expression Analysis of NFATc3 in Normal and Glaucoma LC Cells

Using an antibody against the total (phospho + nonphosphorylated) NFATc3, we found that NFATc3 protein expression was upregulated approximately 4-fold ($n = 3$, $P \leq 0.01$) in glaucoma when compared to that in normal LC cells (Fig. 3A) (although the normal LC donor N2 showed a moderate increase in NFATc3 expression level).

We next determined whether the expression of NFATc3 in normal and glaucoma LC cells was sensitive to an oxidative stress stimulus. LC cells obtained from different normal and glaucoma eye donors were pretreated with H_2O_2 (100 μM) for 6 hours, and the levels of NFATc3 protein expression in treated and nontreated LC cells were assessed using Western blotting analysis. Figures 3B and 3C show that NFAT levels were similarly increased in both normal and glaucoma LC cells following H_2O_2 pretreatment.

Cyclosporin A Reduces the H_2O_2-Induced Increase in NFATc3 Protein Expression, ECM Gene Transcription, and NFATc3 Dephosphorylation

A control experiment was first conducted to determine the effective dose of CsA on NFATc3 expression in H_2O_2-treated normal LC cells. Western blotting analysis using an antibody against the total (phospho + nonphosphorylated) NFATc3 demonstrated that 10 μM CsA pretreatment of normal LC cells inhibited the H_2O_2-induced increase in NFATc3 protein levels (Fig. 4), while low concentrations of CsA (1, 2, 5 μM) failed to block the H_2O_2-induced increase in NFATc3 protein levels. Based on these data, we used 10 μM CsA in all subsequent experiments.

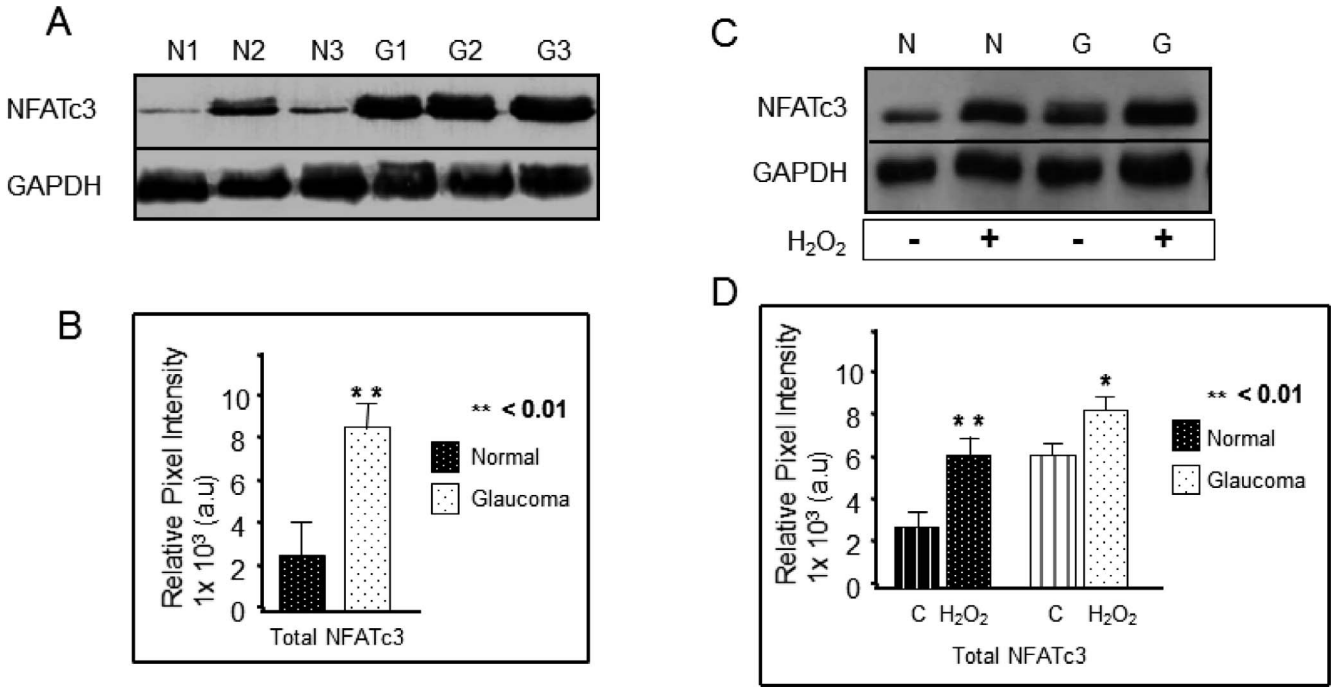

Figure 3. Western blot analysis of NFATc3 expression in normal and glaucoma LC cells. (**A**) Representative example of Western blot analysis of total NFATc3 expression in normal LC cell strains ($n = 3$) and glaucoma cell strains ($n = 3$). Protein lysates were examined for differential expression of the total (phospho + unphosphorylated) NFATc3 protein. Expression of NFATc3 is significantly (**$P < 0.01$) increased in glaucoma (G1, G2, G3) compared to normal control (N1, N2, N3) LC cells. (**B**) Representative illustration of Western blot analysis of NFATc3 expression in normal and glaucoma LC cells exposed (or not) to H_2O_2 (100 μM) for 6 hours to induce a sustained oxidative stress. Note that protein lysates examined showed that the NFATc3 protein expression level is similarly increased by H_2O_2 pretreatment in both normal and glaucoma LC cells. (**C**) Summarized data illustrating the average protein levels of total NFATc3 in two different cell strains for control nontreated and H_2O_2 (100 μM)-treated normal and glaucoma LC cells (**$P < 0.01$, 1-way ANOVA with Tukey-Kramer posttest). Results are expressed as relative pixel intensity versus normal LC samples. GAPDH was used as a loading control. Values that are significantly different from control are denoted by an *asterisk* (*$P < 0.05$, **$P < 0.01$).

We next evaluated whether CsA reduced the profibrotic ECM gene expression. CsA pretreatment significantly reduced H_2O_2-induced expression of the profibrotic ECM genes tested (TGFβ1, Col1A1, and periostin) ($n = 3$, $P < 0.01$) (Fig. 5), both in normal and in glaucoma LC cells.

In a follow-up experiment, we evaluated whether CsA contributes to the profibrotic ECM gene expression through a mechanism involving the Ca^{2+}-calcineurin/NFAT signaling pathway in normal and glaucoma LC cells. Western blotting experiments were performed in untreated controls and H_2O_2-treated normal and glaucoma LC cells in the presence or absence of CsA (10 μM), using an anti-phosphorylated NFATc3 antibody (pNFATc3). Western blot analysis shows that H_2O_2 significantly reduced the phosphorylated NFATc3 expression levels and this reduction was reversed by pretreatment with CsA (Fig. 6). To confirm these results, we used immunofluorescence microscopy to test whether H_2O_2 treatment induced cytoplasmic NFATc3 dephosphorylation and examine whether this dephosphorylation is inhibited by CsA pretreatment. Figure 7 illustrates a decrease in the cytoplasmic levels of phosphorylated NFATc3 when the LC cells were treated with H_2O_2, and this decrease was prevented by pretreating the LC cells with CsA, suggesting that NFATc3 nuclear translocation occurred.

As shown in Supplementary Figure S1, we also found a marked increase in global $[Ca^{2+}]_i$ levels following exposure to 100 μM H_2O_2 in normal LC cells. In CsA-treated normal LC cells, the H_2O_2-mediated elevation of intracellular Ca^{2+} was significantly decreased ($n = 3$, $P < 0.05$).

Discussion

In this study, we found elevated levels of basal and hypotonic cell membrane stretch-induced $[Ca^{2+}]_i$, with delayed reuptake in glaucoma LC cells, and this was associated with increased expression of NFATc3 in glaucoma LC cells. Both normal and glaucoma LC cells were sensitive to an oxidative stress stimulus. Pretreatment with CsA significantly reduced fibrosis gene (TGFβ1, Col1A1, and periostin) expression and reversed the H_2O_2-induced reduction in p-NFATc3 both in normal and in glaucoma LC cells.

Changes in cytosolic Ca^{2+} concentration play a vital role in intracellular signaling pathways related to proliferation, differentiation, apoptosis, and gene expression.[40] In normal cells, the intracellular Ca^{2+} concentration is tightly regulated and kept relatively constant through a variety of homeostatic mechanisms.[40] Ca^{2+} influx from the extracellular space and Ca^{2+} release from the intracellular sources determine the $[Ca^{2+}]_i$. We previously used single-wavelength flow cytometry (which is most useful for quantitative measurements of $[Ca^{2+}]_i$ in a population of cells) to show that intracellular Ca^{2+} levels were higher in glaucoma LC cells compared to normal controls.[12,39] In our current study, we used the radiometric dual-wavelength indicator Fura 2-AM (which has the advantage that it can be used for both quantitative and qualitative data) to measure changes in $[Ca^{2+}]_i$.[35] Extracellular Ca^{2+} influx and/or release of Ca^{2+} from intracellular stores are the two sources of increased $[Ca^{2+}]_i$. We first examined whether this elevated cytosolic Ca^{2+} in glaucoma LC cells could have resulted from extracellular Ca^{2+} influx. We found that introduction of extracellular Ca^{2+} to the bathing solution increased $[Ca^{2+}]_i$ in

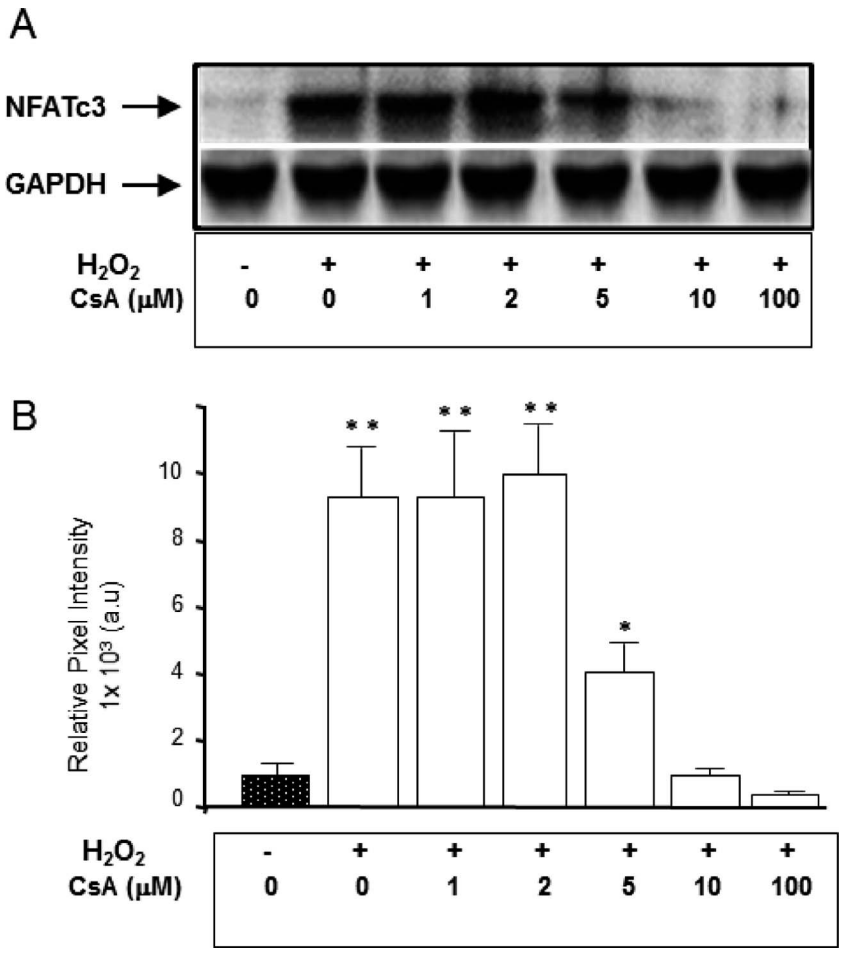

FIGURE 4. Effect of cyclosporin A on H_2O_2-induced NFATc3 expression in normal LC cells. LC cells were preincubated overnight with different concentrations of CsA (0, 1, 2, 5, 10, 100 μM) and cultured at 37°C with or without H_2O_2 (100 μM) for 6 hours to induce a sustained oxidative stress. (**A**) Representative Western immunoblotting performed using an anti-NFATc3–specific antibody. (**B**) Summarized data of total NFATc3 expression in three different LC cell strains. Note that CsA 10 μM completely blocked NFATc3 expression. Results are expressed as relative pixel intensity versus control LC samples. GAPDH was used as a loading control. Values significantly different from control are denoted by an *asterisk* (*$P < 0.05$, **$P < 0.01$).

both basal and hypotonic cell stretch conditions, and this increase was more pronounced in glaucoma compared to normal LC cells (Fig. 1). The LC cell response to hypotonic stretch in the presence of extracellular Ca^{2+} was a typical response characterized by an initial Ca^{2+} transient spike phase, which is generated by inositol trisphosphate receptor (IP3-R)-dependent Ca^{2+} release from the intracellular stores.[40] The resulting depletion of the Ca^{2+} stores by TG generates the activation of several types of cation channels such as store-operated channels, leading to the sustained $[Ca^{2+}]_i$ increase by initiating extracellular Ca^{2+} influx.[40]

Having demonstrated the contribution of extracellular Ca^{2+} to the abnormally raised $[Ca^{2+}]_i$ in glaucoma LC cells, we next tested whether the release of Ca^{2+} from intracellular stores could also contribute to the abnormally elevated levels of $[Ca^{2+}]_i$ found in glaucoma LC cells. Therefore, we experimentally separated intracellular Ca^{2+} release from extracellular Ca^{2+} influx. The first part of the experiment (Fig. 2) showed that the release of Ca^{2+} from intracellular stores also contributed to the defective Ca^{2+} homeostasis found in glaucoma LC cells, as removal of the residual external Ca^{2+} from the external medium with EGTA followed by TG application resulted in a transient rise of $[Ca^{2+}]_i$, with similar amplitudes in glaucoma and normal LC cells. However, in normal LC cells, the $[Ca^{2+}]_i$ returned to basal levels approximately 2 minutes after TG application, while return to baseline took 12 to 14 minutes in the glaucoma cells, indicating a lack of refilling of intracellular stores in glaucoma LC cells. These results complement our previous work, where an increase in SERCA2 and SERCA3 protein expression levels was observed in glaucoma LC cells.[12] Interestingly, the second part of the experiment (Fig. 2) showed that the addition of extracellular Ca^{2+} to the hypotonic buffer markedly increased the Ca^{2+} amplitude of the sustained phase of Ca^{2+} elevation more in the glaucoma than in normal LC cells. This suggests that the Ca^{2+} entry channels are operating in a high open probability gating mode,[40] thus generating persistent Ca^{2+} influx in glaucoma LC cells. Furthermore, and more importantly, the normal LC cells recovered to baseline Ca^{2+} levels in contrast to the glaucoma LC cells after changing back to isotonic solution, suggesting a defect of Ca^{2+} extrusion from the intracellular space. The key components that maintain stable Ca^{2+} gradients in cells are believed to be plasma membrane Ca^{2+} entry channels, ATP-driven pumps (PMCAs), electrogenic exchangers Na^+-Ca^{2+} (NCX), and SERCA pumps.[40] In our previous study,[12] we also found that the Ca^{2+} extrusion system is altered in glaucoma LC cells. Our data showed that NCX expression levels were significantly lower in glaucoma LC cells, suggesting a defect in Ca^{2+} extrusion from the intracellular space.[12]

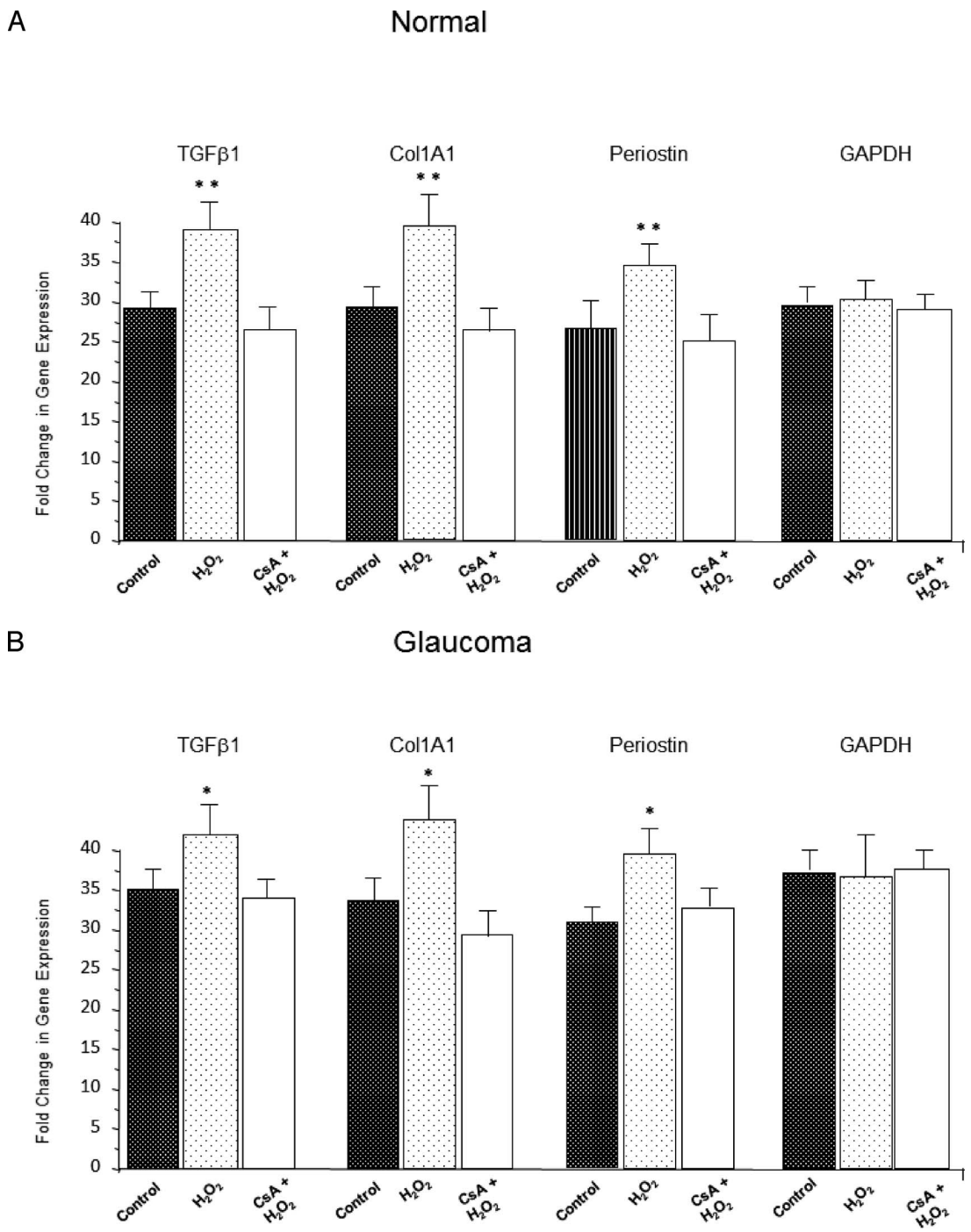

FIGURE 5. Effect of cyclosporin A on H_2O_2-induced profibrotic gene transcription in LC cells. Normal (**A**) and glaucoma (**B**) LC cells treated with H_2O_2 (100 μM) for 6 hours with or without CsA (10 μM overnight prior to H_2O_2 stimulation). The expression of TGFβ1, Col1A1, and periostin mRNA was assessed by quantitative real-time RT-PCR analysis. H_2O_2 significantly increased profibrotic gene expression of the ECM genes tested, and this increase was significantly blocked following CsA pretreatment (**$P < 0.01$, 2-tailed unpaired Student's *t*-test). The summary data are from LC cells obtained from three normal control eye donors ($N = 3$) and three glaucoma eye donor patients ($N = 3$). Data were normalized to GAPDH, which had the same level of expression in normal nonstressed and normal stressed LC cells.

Our results showing elevated $[Ca^{2+}]_i$ levels in glaucoma LC cells are very similar to findings in TM cells.[37] There is strong evidence of increased ECM production in the glaucomatous TM[41] resulting in a reduced outflow facility. The paper by He and colleagues[37] shows an increase in cytosolic and mitochondrial Ca^{2+} in primary open-angle glaucoma (POAG) TM cells with evidence of mitochondrial dysfunction. The link between the anterior and posterior segments in glaucoma was well discussed in a recent review paper by Sacca and colleagues.[42] Of interest also are papers by Sappington et al.[43] and Niittykoski et al.,[44] who also demonstrated increased $[Ca^{2+}]_i$ levels in glaucomatous retinal ganglion cells (RGC).[43,44] Other work in a rodent ocular hypertension model showed that calcineurin is activated in RGCs and participates in RGC death,[45] which was prevented by CsA treatment.[45]

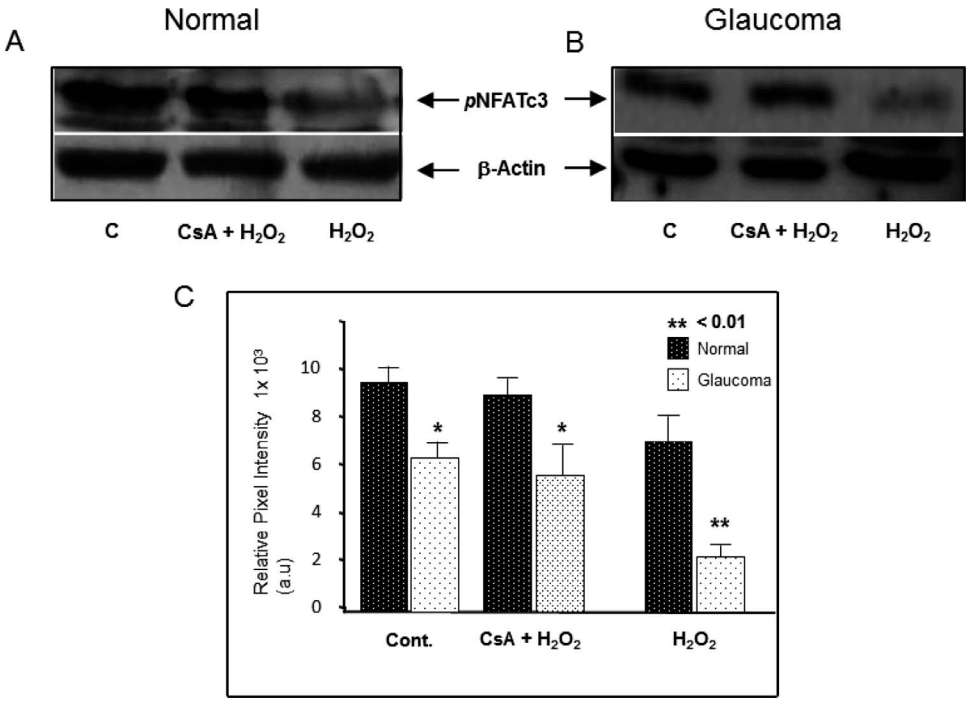

Figure 6. Effect of cyclosporin A on H_2O_2-induced NFATc3 protein dephosphorylation in lamina cribrosa cells. Western blot analysis of NFATc3 protein dephosphorylation in normal and glaucoma lamina cribrosa cells. Phosphorylated NFATc3 (pNFATc3) protein expression in normal (**A**, *top left*) and glaucoma (**B**, *top right*), nontreated controls, or H_2O_2-treated LC cells (100 μM) for 6 hours in absence or presence of the calcineurin blocker CsA (10 μM). (**C**) Histograms summarizing data from the phosphorylated pNFATc3 expression levels in LC cells obtained from three normal and three glaucoma age-matched eye donors. Note that CsA (10 μM) significantly blocked the H_2O_2-induced dephosphorylation of NFATc3, both in normal and in glaucoma LC cells (**$P < 0.01$, 1-way ANOVA with Tukey-Kramer posttest). Results are expressed as relative pixel intensity versus control LC samples. GAPDH was used as a loading control, with the same level of expression seen in nonstressed and stressed cell lysates. Values significantly different ($P < 0.05$) from control are denoted by an *asterisk*.

Cellular responses to Ca^{2+} mobilization are highly versatile due to the capacity of intracellular Ca^{2+} signaling to activate an extensive repertoire of downstream signaling targets,[40] including NFAT and other pathways such as PKCα and MAPK. Consequently, any long-term increase in $[Ca^{2+}]_I$ will have larger knock-on effects in the intracellular signaling pathways, and we believe that the small but statistically significant increase in baseline $[Ca^{2+}]_I$ will have a larger impact on, for example, the NFAT pathway as shown in Figure 3.

In addition, intracellular Ca^{2+} levels play a key role in neurodegenerative diseases. Several lines of evidence indicate that intracellular Ca^{2+} levels are elevated in Alzheimer's disease.[46] A rise in $[Ca^{2+}]_i$ levels results in subsequent defects in neuronal Ca^{2+} signaling. Altered Ca^{2+} signals shift the balance between Ca^{2+}-dependent phosphatase calcineurin and

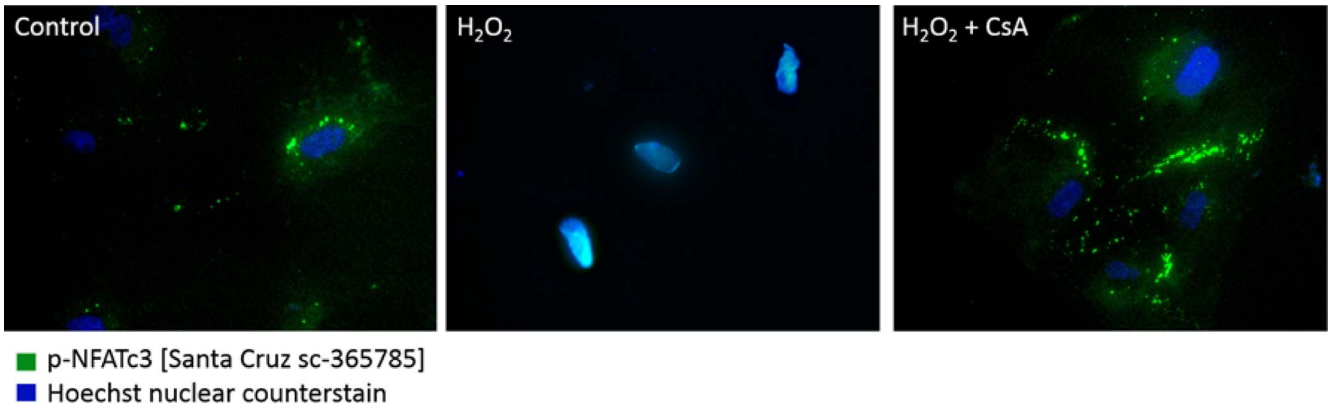

Figure 7. Effect of cyclosporin A on H_2O_2-induced NFATc3 nuclear translocation in lamina cribrosa cells. Human LC cells were grown on the Nunc Lab-Tek II Chamber Slide System until 60% to 70% confluent and starved in serum-free medium for 24 hours. The serum-free medium was then removed, and cells were subjected to oxidative stress using H_2O_2 at 37°C in the presence or absence of CsA. Cells were then fixed with methanol (100%), and immunofluorescence microscopy was performed to determine the NFATc3 phosphorylation using phosphorylated NFATc3 antibody. Immunofluorescence images were taken before (control) and after addition of H_2O_2 (100 μM) with or without CsA pretreatment. Note that H_2O_2 treatment induced a decrease in the cytoplasmic levels of phosphorylated NFATc3 and this decrease was inhibited when LC cells were pretreated with CsA (10 μM).

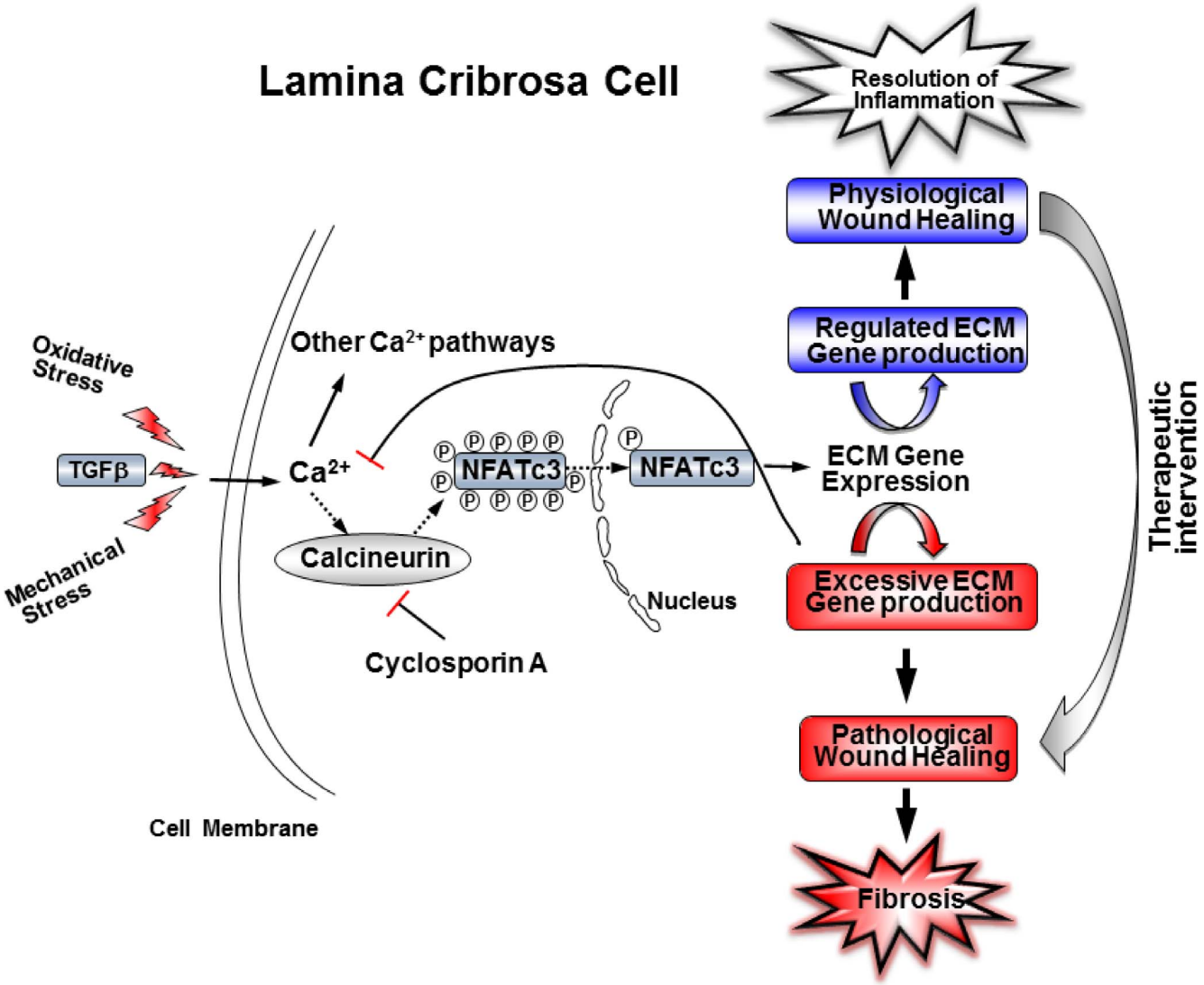

Figure 8. Proposed mechanism of profibrotic gene transcription regulation via the calcineurin/nuclear factor of the activated T cells (NFATc3) signaling pathway in LC cells. Intracellular Ca^{2+} levels increase in response to stimuli such as TGFβ, oxidative stress, and cell membrane stretch resulting in calmodulin saturation, which in turn promotes calcineurin activation. Activated calcineurin dephosphorylates several substrates, including the NFAT transcription factors, which then translocate from the cytoplasm to the nucleus and activate Ca^{2+}-inducible genes including those contributing to fibrosis in glaucoma. CsA inhibits calcineurin activation, thereby preventing NFAT dephosphorylation and inhibiting fibrosis. In LC cells, this include ECM genes, the protein products of which inhibit calcineurin, resulting in a negative feedback loop.

Ca^{2+}/calmodulin-dependent protein kinase II (CaMKII), which are extremely abundant in synaptic locations. A change in the balance of CaMKII and calcineurin activity causes synaptic and memory damage that subsequently lead to synaptic loss and neurodegeneration. Despite the differences in mechanisms of cell loss, most of the neurodegenerative disorders share some common characteristics, including the contribution of mitochondrial dysfunction and oxidative stress in the development of pathology and, specific for each disease, misfolded proteins that aggregate in the brain.[47] Being the main energy producer in the cell, mitochondria play an important role in the mechanism of apoptosis, Ca^{2+}, and redox signaling.[48] The ability of mitochondria to produce reactive oxygen species (ROS) in the electron transport chain has a functional consequence in cell signaling; nevertheless, overproduction of ROS in mitochondria links this organelle to age-related pathology and neurodegenerative disorders.[49] In addition, mitochondria also provide a direct link between environment and genes.[50]

We consequently examined and compared the NFATc3 isoform protein expression between normal controls and glaucoma LC cells. NFATc3 protein expression is upregulated approximately 4-fold ($P \leq 0.01$) in glaucoma LC cells. In addition, both normal and glaucoma LC cells were sensitive to an oxidative stress (H_2O_2) stimulus, as the NFATc3 protein expression levels were similarly increased in both normal and glaucoma LC cells following H_2O_2 treatment. NFAT is a Ca^{2+}-dependent transcription factor that regulates the expression of specific genes through a calcineurin-dependent signaling pathway in various cell types.[19] The NFAT family of transcription factors are highly phosphorylated in the cytoplasm of resting cells. However, an increase of $[Ca^{2+}]_i$ levels triggers the opening of ion channels in the plasma membrane, allowing extracellular Ca^{2+} influx that activates calcineurin.[20] Calcineurin dephosphorylates NFATc3 to allow its nuclear translocation and ultimately activates Ca^{2+}-dependent gene transcription, including profibrotic ECM genes.[17,18,21,23]

Given the extensive number of studies demonstrating a key role for NFAT in driving hypertrophic gene expression in cardiac tissues and fibrosis,[17–23] we speculate that NFAT plays a similar role in LC cells in glaucoma. In addition to its role in the immune system and cardiac tissues, NFATc3 plays a key role in activating the Ca^{2+}/calmodulin/calcineurin/NFAT signaling pathway in pulmonary arterial smooth muscle cells in models of pulmonary hypertension.[51–53]

In the present study, our findings revealed that the blockade of NFATc3 activation with CsA resulted in the downregulation of H_2O_2-induced profibrotic gene expression including TGFβ1, Col1A1, and periostin in normal and glaucoma LC cells. We also demonstrated that CsA pretreatment significantly reversed the H_2O_2 reduction in phosphorylated NFAT and its nuclear translocation, indicating that CsA reduces the H_2O_2-induced profibrotic gene expression through a mechanism involving the Ca^{2+}/calcineurin/NFAT signaling pathway in normal and glaucoma LC cells.

In addition, we further examined the effect of CsA on H_2O_2-induced elevation on "global" $[Ca^{2+}]_i$ levels using confocal imaging where the LC cells were loaded with Fluo-4 to detect cytoplasmic Ca^{2+} changes (Supplementary Fig. S1). Treatment of LC cells with CsA resulted in a significant reduction of the global cytosolic Ca^{2+} induced by oxidative stress in normal LC cells.

In the present study, we utilized two glaucoma-related stimuli (oxidative stress and hypo-osmotic cell membrane stretch) to assess calcium homeostasis in LC cells. Previous glaucoma investigations have identified a key role for oxidative stress[37,54] and cell stretch.[39,55] Oxidative and osmotic stress differ significantly, although they display overlapping molecular and signaling responses. In general, oxidative stress is caused by the intracellular accumulation of ROS or a disturbance of the cellular redox state.[56] Oxidative stress signals may come from the environment, but can also be generated internally and may cause molecular damage to protein DNA and membranes.[56] Oxidative stress is associated with mitochondrial dysfunction and elevated cytosolic and mitochondrial calcium in cardiac and other forms of fibrosis.[57] Osmotic stress, however, leads to efflux or influx of water from or into the cell: hyperosmotic stress causes cell shrinking, while hypo-osmotic stress causes cell membrane stretch, calcium influx,[58] and cell swelling. Both stimuli have been shown to activate growth factor expression[59,60] and profibrotic ECM proteins.[61,62]

In conclusion, we found elevated NFAT expression in glaucoma LC cells. CsA inhibited the oxidative stress–induced increase in NFAT expression and transcription activity and also ECM profibrotic gene expression in normal and glaucoma LC cells. This suggests that inhibition of the NFAT signaling pathway may reduce LC fibrosis in glaucoma (Fig. 8).

Acknowledgments

Supported by the 2014 Shaffer Grants for Innovative Glaucoma Research Foundation.

Disclosure: **M. Irnaten**, None; **A. Zhdanov**, None; **D. Brennan**, None; **T. Crotty**, None; **A. Clark**, None; **D. Papkovsky**, None; **C. O'Brien**, None

References

1. Quigley HA, Broman AT. The number of people with glaucoma worldwide in 2010 and 2020. *Br J Ophthalmol*. 2006;90:262–267.
2. Quigley HA, Hohman RM, Addicks EM, et al. Morphological changes in the lamina cribrosa correlated with neural loss in open-angle glaucoma. *Am J Ophthalmol*. 1983;95:673–691.
3. Hernandez MR, Andrzejewska WM, Neufeld AH. Changes in the extracellular matrix of the human optic nerve head in primary open-angle glaucoma. *Am J Ophthalmol*. 1990;109:180–188.
4. Pena JD, Taylor AW, Ricard CS, et al. Transforming growth factor beta isoforms in human optic nerve heads. *Br J Ophthalmol*. 1999;83:209–218.
5. Zode GS, Sethi A, Brun-Zinkernagel AM, et al. Transforming growth factor-β2 increases extracellular matrix proteins in optic nerve head cells via activation of the Smad signaling pathway. *Mol Vis*. 2011;17:1745–1758.
6. Wynn TA. Cellular and molecular mechanisms of fibrosis. *J Pathol*. 2008;214:199–210.
7. Tomasek JJ, Gabbiani G, Hinz B, Chaponnier C, Brown RA. Myofibroblasts and mechano-regulation of connective tissue remodelling. *Nat Rev Mol Cell Biol*. 2002;3:349–363.
8. Leask A. Potential therapeutic targets for cardiac fibrosis: TGFbeta, angiotensin, endothelin, CCN2, and PDGF, partners in fibroblast activation. *Circ Res*. 2010;106:1675–1680.
9. Van den Borne SW, Diez J, Blankesteijn WM, et al. Myocardial remodeling after infarction: the role of myofibroblasts. *Nat Rev Cardiol*. 2010;7:30–37.
10. Hinz B. The extracellular matrix and transforming growth factor-β1: tale of a strained relationship. *Matrix Biol*. 2015;47:54–65.
11. Kirwan RP, Leonard MO, Murphy M, et al. Transforming growth factor-beta-regulated gene transcription and protein expression in human GFAP-negative lamina cribrosa cells. *Glia*. 2005;52:309–324.
12. McElnea EM, Quill B, Docherty NG, et al. Oxidative stress, mitochondrial dysfunction and calcium overload in human lamina cribrosa cells from glaucoma donors. *Mol Vis*. 2011;17:1182–1191.
13. Rao VR, Krishnamoorthy RR, Yorio T. Endothelin-1 mediated regulation of extracellular matrix collagens in cells of human lamina cribrosa. *Exp Eye Res*. 2008;86:886–894.
14. Desmoulière A. Factors influencing myofibroblast differentiation during wound healing and fibrosis. *Cell Biol Int*. 1995;19:471–476.
15. Diegelmann RF, Evans MC. Wound healing: an overview of acute, fibrotic and delayed healing. *Front Biosci*. 2004;9:283–289.
16. Frey N, McKinsey TA, Olson EN. Decoding calcium signals involved in cardiac growth and function. *Nat Med*. 2000;6:1221–1227.
17. Molkentin JD. Calcineurin–NFAT signaling regulates the cardiac hypertrophic response in coordination with the MAPKs. *Cardiovasc Res*. 2004;63:467–475.
18. Wilkins BJ, Dai YS, Bueno OF, et al. Calcineurin/NFAT coupling participates in pathological, but not physiological, cardiac hypertrophy. *Circ Res*. 2004;94:110–118.
19. Macian F. NFAT proteins: key regulators of T-cell development and function. *Nat Rev Immunol*. 2005;5:472–484.
20. Maldonado-Pérez D, Brown P, Morgan K, et al. Prokineticin 1 modulates IL-8 expression via the calcineurin/NFAT signaling pathway. *Biochim Biophys Acta*. 2009;1793:1315–1324.
21. Hogan PG, Chen L, Nardone J, Rao A. Transcriptional regulation by calcium, calcineurin, and NFAT. *Genes Dev*. 2003;17:2205–2232.
22. Bootman MD, Fearnley C, Smyrnias I, et al. An update on nuclear calcium signaling. *J Cell Sci*. 2009;122(pt 14):2337–2350.
23. Nieves-Cintrón M, Amberg GC, Navedo MF, et al. The control of Ca2+ influx and NFATc3 signaling in arterial smooth muscle during hypertension. *Proc Natl Acad Sci U S A*. 2008;105:15623–15628.

24. Houser SR, Molkentin JD. Does contractile Ca^{2+} control calcineurin-NFAT signaling and pathological hypertrophy in cardiac myocytes? *Sci Signal*. 2008;1:pe31.
25. Timmerman LA, Clipstone NA, Ho SN, et al. Rapid shuttling of NF-AT in discrimination of Ca^{2+} signals and immunosuppression. *Nature*. 1996;383:837–840.
26. Weinblatt ME, Coblyn JS, Fraser PA, et al. Cyclosporin A treatment of refractory rheumatoid arthritis. *Arthritis Rheum*. 1987;30:11–17.
27. Kokado Y, Takahara S, Kyo M, et al. Low-dose tacrolimus (FK506)-based immunosuppressive protocol in living donor renal transplantation. *Transpl Int*. 1998;11(suppl 1):S60–S64.
28. Kacmaz RO, Kempen JH, Newcomb C, et al. Cyclosporine for ocular inflammatory diseases. *Ophthalmology*. 2010;117:576–584.
29. Shii D, Nakagawa S, Shinomiya K, et al. Cyclosporin A eye drops inhibit fibrosis and inflammatory cell infiltration in murine type I allergic conjunctivitis without affecting the early-phase reaction. *Curr Eye Res*. 2009;34:426–437.
30. Guzey M, Karaman SK, Satici A, et al. Efficacy of topical cyclosporine A in the treatment of severe trachomatous dry eye. *Clin Exp Ophthalmol*. 2009;37:541–549.
31. Irnaten M, Barry RC, Wallace DM, et al. Elevated maxi-K^+ ion channel current in glaucomatous lamina cribrosa cells. *Exp Eye Res*. 2013;115:224–229.
32. Irnaten M, Barry RC, Quill B, et al. Activation of stretch-activated channels and maxi-K^+ channels by membrane stress of human lamina cribrosa cells. *Invest Ophthalmol Vis Sci*. 2009;50:194–202.
33. Kirwan RP, Wordinger RJ, Clark AF, O'Brien CJ. Differential global and extra-cellular matrix focused gene expression patterns between normal and glaucomatous human lamina cribrosa cells. *Mol Vis*. 2009;15:76–88.
34. Lambert W, Agarwal R, Howe W, Clark AF, Wordinger RJ. Neurotrophin and neurotrophin receptor expression by cells of the human lamina cribrosa. *Invest Ophthalmol Vis Sci*. 2001;42:2315–2323.
35. Grynkiewicz G, Poenie M, Tsien RY. A new generation of Ca2+ indicators with greatly improved fluorescence properties. *J Biol Chem*. 1985;260:3440–3450.
36. Wimmers S, Strauss O. Basal calcium entry in retinal pigment epithelial cells is mediated by TRPC channels. *Invest Ophthalmol Vis Sci*. 2007;48:5767–5772.
37. He Y, Ge J, Tombran-Tink J. Mitochondrial defects and dysfunction in calcium regulation in glaucomatous trabecular meshwork cells. *Invest Ophthalmol Vis Sci*. 2008;49:4912–4922.
38. Livak KJ, Schmittgen TD. Analysis of relative gene expression data using real-time quantitative PCR and the $2^{-\Delta\Delta CT}$ method. *Methods*. 2001;25:402–408.
39. Quill B, Irnaten M, Docherty NG, et al. Calcium channel blockade reduces mechanical strain-induced extracellular matrix gene response in lamina cribrosa cells. *Br J Ophthalmol*. 2015;99:1009–1014.
40. Berridge MJ, Bootman MD, Roderick HL. Ca^{2+} signaling: dynamics, homeostasis and remodelling. *Nat Rev Mol Cell Biol*. 2003;4:517–529.
41. Vranka JA, Kelley MJ, Acott TS, Keller KE. Extracellular matrix in the trabecular meshwork: intraocular pressure regulation and dysregulation in glaucoma. *Exp Eye Res*. 2015;133:112–125.
42. Sacca SC, Gandolfi S, Bagnis A, et al. From DNA damage to functional changes of the trabecular meshwork in aging and glaucoma. *Ageing Res Rev*. 2016;29:26–41.
43. Sappington RM, Sidorova T, Long DJ, Calkins DJ. TRPV1: contribution to retinal ganglion cell apoptosis and increased intracellular Ca2+ with exposure to hydrostatic pressure. *Invest Ophthalmol Vis Sci*. 2009;50:717–728.
44. Niittykoski M, Kalesnykas G, Larsson KP, et al. Altered calcium signaling in an experimental model of glaucoma. *Invest Ophthalmol Vis Sci*. 2010;51:6387–6393.
45. Huang W, Fileta JB, Dobberfuhl A, et al. Calcineurin cleavage is triggered by elevated intraocular pressure, and calcineurin inhibition blocks retinal ganglion cell death in experimental glaucoma. *Proc Natl Acad Sci U S A*. 2005;102:12242–12247.
46. Magi S, Castaldo P, Macrì ML, et al. Intracellular calcium dysregulation: implications for Alzheimer's disease. *Biomed Res Int*. 2016;2016:6701324.
47. Shah SZ, Hussain T, Zhao D, Yang L. A central role for calcineurin in protein misfolding neurodegenerative diseases. *Cell Mol Life Sci*. 2017;74:1061–1074.
48. Burchell VS, Gandhi S, Deas E, Wood NW, Abramov AY, Plun-Favreau H. Targeting mitochondrial dysfunction in neurodegenerative disease: part I. *Expert Opin Ther Targets*. 2010;14:369–385.
49. Angelova PR, Abramov AY. Functional role of mitochondrial reactive oxygen species in physiology. *Free Radic Biol Med*. 2016;100:81–85.
50. Wallace DC. A mitochondrial paradigm of metabolic and degenerative diseases, aging, and cancer: a dawn for evolutionary medicine. *Annu Rev Genet*. 2005;39:359–407.
51. Ermak G, Davies KJ. Calcium and oxidative stress: from cell signaling to cell death. *Mol Immunol*. 2002;38:713–721.
52. De Frutos S, Spangler R, Alò D, Bosc LV. NFATc3 mediates chronic hypoxia-induced pulmonary arterial remodeling with alpha-actin up-regulation. *J Biol Chem*. 2007;282:15081–15089.
53. De Frutos S, Caldwell E, Nitta CH, et al. NFATc3 contributes to intermittent hypoxia-induced arterial remodelling in mice. *Am J Physiol Heart Circ Physiol*. 2010;299:H356–H363.
54. Saccà SC, Pascotto A, Camicione P, Capris P, Izzotti A. Oxidative DNA damage in the human trabecular meshwork: clinical correlation in patients with primary open-angle glaucoma. *Arch Ophthalmol*. 2005;123:458–463.
55. Keller KE, Kelley MJ, Acott TS. Extracellular matrix gene alternative splicing by trabecular meshwork cells in response to mechanical stretching. *Invest Ophthalmol Vis Sci*. 2007;48:1164–1172.
56. Ferreira M, Moradas-Ferreira P, Reis-Henriques MA. Oxidative stress biomarkers in two resident species, mullet (Mugil cephalus) and flounder (Platichthys flesus), from a polluted site in River Douro Estuary, Portugal. *Aquat Toxicol*. 2005;71:39–48.
57. Shahbaz AU, Sun Y, Bhattacharya SK, et al. Fibrosis in hypertensive heart disease: molecular pathways and cardioprotective strategies. *J Hypertens*. 2010;28(suppl 1):S25–S32.
58. Christensen O. Mediation of cell volume regulation by Ca2+ influx through stretch-activated channels. *Nature*. 1987;330:66–68.
59. Zhang P, Xing K, Randazzo J, Blessing K, Lou MF, Kador PF. Osmotic stress, not aldose reductase activity, directly induces growth factors and MAPK signaling changes during sugar cataract formation. *Exp Eye Res*. 2012;101:36–43.
60. Veltmann M, Hollborn M, Reichenbach A, Wiedemann P, Kohen L, Bringmann A. Osmotic induction of angiogenic growth factor expression in human retinal pigment epithelial cells. *PLoS One*. 2016;11:e0147312.
61. Dihazi H, Dihazi GH, Mueller C, et al. Proteomics characterization of cell model with renal fibrosis phenotype: osmotic stress as fibrosis triggering factor. *J Proteomics*. 2011;74:304–318.
62. Liu RM, Desai LP. Reciprocal regulation of TGF-β and reactive oxygen species: a perverse cycle for fibrosis. *Redox Biol*. 2015;6:565–577.

Investigative Ophthalmology & Visual Science